

## Supplementary Information

### **Tailoring the spatial localization of bound state in the continuum in plasmonic-dielectric hybrid system**

Jin Xiang,<sup>1</sup> Yi Xu,<sup>2\*</sup> Jingdong Chen,<sup>3</sup> and Sheng Lan<sup>1\*</sup>

<sup>1</sup>*Guangdong Provincial Key Laboratory of Nanophotonic Functional Materials and Devices, School of Information and Optoelectronic Science and Engineering, South China Normal University, Guangzhou 510006, China*

<sup>2</sup>*Department of Electronic Engineering, College of Information Science and Technology, Jinan University, 510632 Guangzhou, China.*

<sup>3</sup>*College of Physics and Information Engineering, Minnan Normal University, Zhangzhou 363000, China*

\*Corresponding Author: [yi.xu@osamember.org](mailto:yi.xu@osamember.org), [slan@scnu.edu.cn](mailto:slan@scnu.edu.cn)

### **Table of contents**

<b>1. Revealing the resonant modes in all-dielectric and hybrid structures.....</b>	<b>2</b>
<b>2. Influence of the dipole-source location on the resonant wavelength.....</b>	<b>2</b>
<b>3. Dependence of the effective mode volume on the gap width.....</b>	<b>3</b>
<b>4. The distribution of electric field components of symmetry protected BICs...4</b>	
<b>5. The corresponding reflection spectra calculated using the refractive index of silicon measured from experiment.....</b>	<b>4</b>

## 1. Revealing the resonant modes in all-dielectric and hybrid structures

Since symmetry-protected BIC does not couple with the plane wave normally incident on the all-dielectric and hybrid structures, we used randomly distributed 10 electric dipole sources inside the structure to excite such mode and record the time evolution in 7 random locations inside the structure for further modal analysis. We perform FFT of all time domain signals to reveal the resonant modes of the hybrid structures. In Figure S1a, we show the evolutions of the electric field in time domain recorded at 7 randomly distributed locations in the hybrid structure. The Fourier transform results of the time-domain signals into the frequency domain are presented in Fig. S1b. The relative amplitude of a resonant mode is taken as the averaged value of all FFT results. By taking average of these results, the resonant modes in hybrid structures and all-dielectric structures with different lattice constants can be qualitatively extracted, as shown in Figs. 2a, 6a and d.

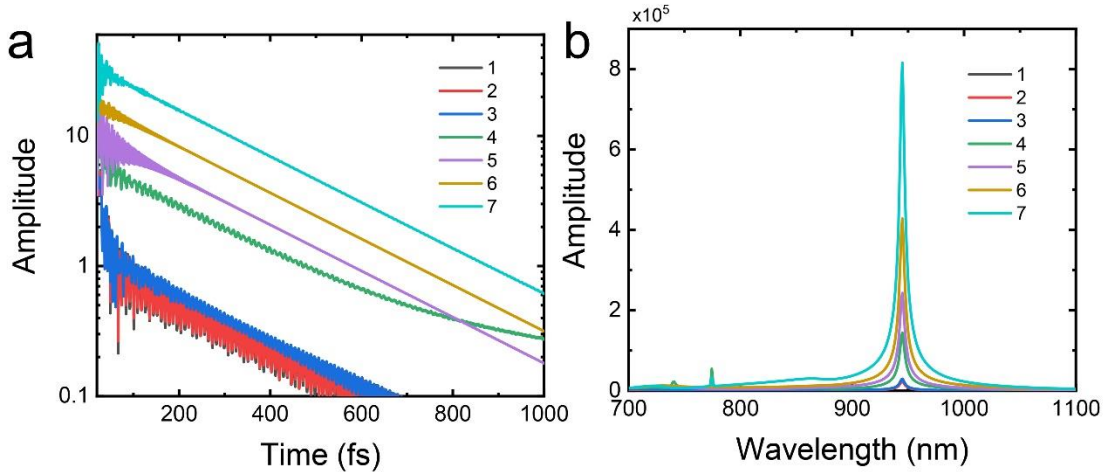


**Figure S1** (a) Decays of the signals in time domain detected at 7 locations randomly distributed in a hybrid structure.

(b) Fourier transform results of the time-domain signals into the frequency domain.

## 2. Influence of the dipole-source location on the resonant wavelength

As discussed above, we used randomly oriented and distributed electric dipole sources to excite the resonant modes of a hybrid structure and record the time evolutions of 7 randomly chosen locations to extract the resonant wavelengths of these resonant modes. In order to find out the influence of the dipole-source location on the extracted resonant wavelength, we examined different realizations of the electric dipole sources and a comparison of two typical

cases is presented in Fig. S2. In each case, ten randomly oriented and distributed dipole sources were employed, as shown in Fig. S2a. As can be seen in Fig. S2b, the resonant wavelengths of the modes extracted by using two realizations of dipole sources are almost the same, implying that the dipole-source localizations have negligible influence on the extracted resonant wavelengths provided that the numbers of dipole sources are sufficient.

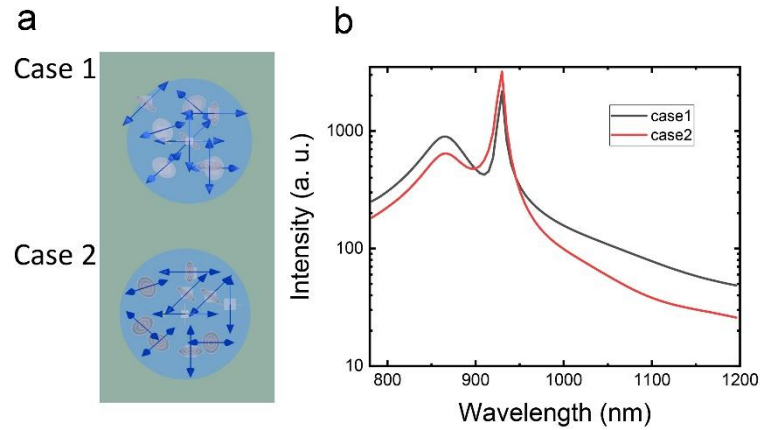


**Figure S2** (a) Two realizations of randomly oriented and distributed electric dipole sources in the Si nanopillar used to excite the resonant modes of the hybrid structure. (b) Resonant wavelengths of the excited modes extracted from the time-domain signals.

### 3. Dependence of the effective mode volume on the gap width

As discussed in the main text, the electric field is strongly localized in the gap region between the Si nanopillar and the Ag film for the symmetry-protected BIC. In this case, the mode volume exhibits a strong dependence on the gap width ( $g$ ). In order to gain a deep insight into the manipulation of electric field localization in the symmetry-protected BIC, we calculated the electric field distributions for hybrid structures with different gap widths, as shown in Fig. S3. It is noticed that the electric field is strongly localized in the nanoscale spacer region between the Si nanopillar and the Ag film, leading to a reduction of the effective mode volume in the unit cell of the structure together with decreasing the gap width.

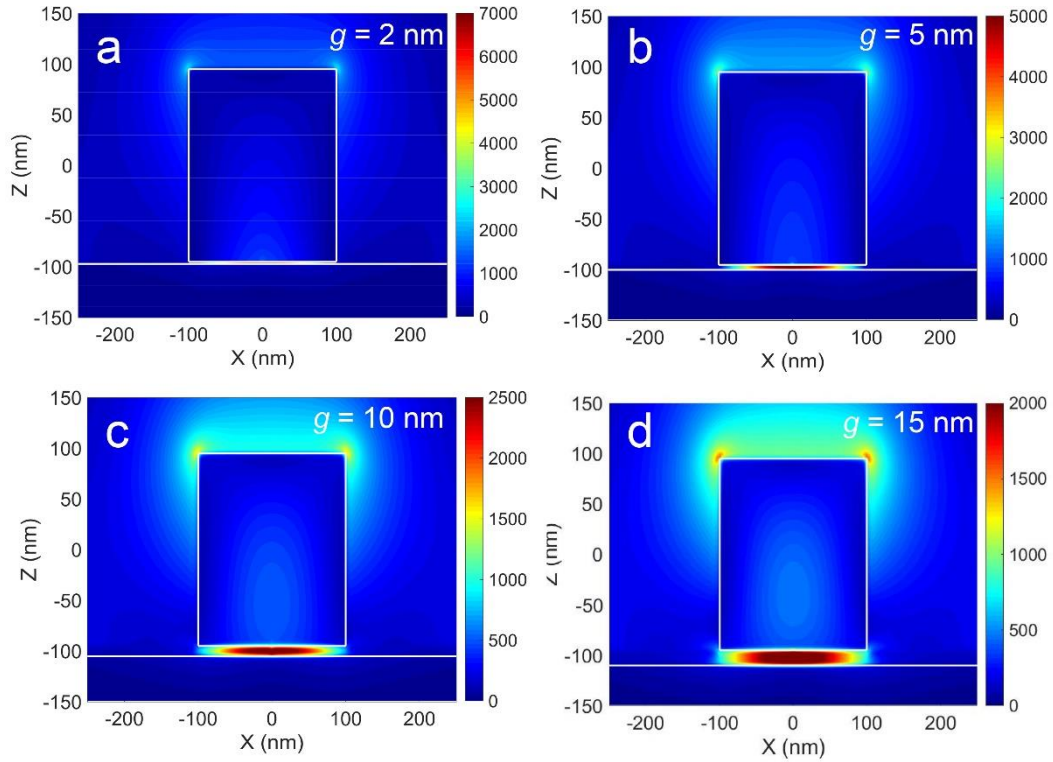


**Figure S3** Electric field distributions calculated for hybrid structures with the same diameter and height for Si nanopillars ( $d = 200$  nm,  $h = 190$  nm) and different gap widths. The gap value of the structure is shown in the inset.

#### 4. The distribution of electric field components of symmetry protected BICs.

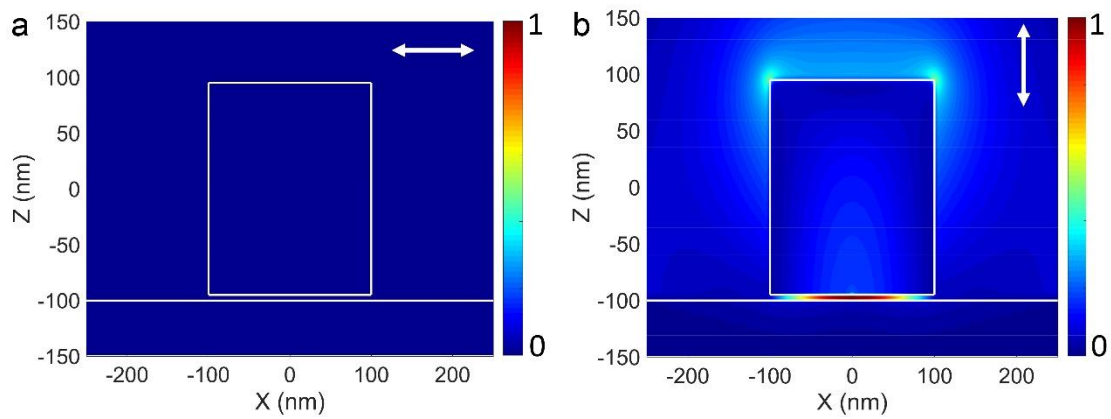


**Figure S4** The distributions of X and Z components of electric field at the central XZ plane calculated for the SPBIC mode of the hybrid structure with the lattice constant  $l = 700$  nm.

#### 5. The corresponding reflection spectra calculated using the refractive index of silicon measured from experiment

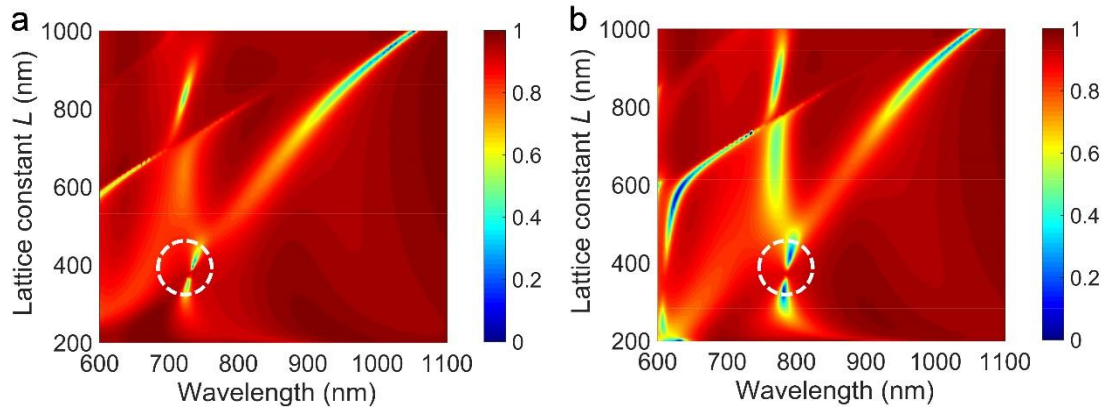


**Figure S5** (a) Resonant modes revealed in the reflection spectra of a normally incident plane wave calculated for hybrid structures with different lattice constants. In this case, the refractive index of Si is set to be  $n=3.4$ . (b) The same results while the refractive index of Si measured from experiment is used.